

Spectral Characteristics of Aqueous Dispersions Enriched in Oxygen

O. A. Novruzova

*Institute of Industrial Ecology, Ural Division, Russian Academy of Sciences,
ul. Sof'i Kovalevskoi 20a, Yekaterinburg, 620219 Russia
e-mail: galashev@ecko.uran.ru*

Received June 15, 2006

Abstract—The IR absorption and reflection spectra of aqueous dispersions consisting of $(\text{H}_2\text{O})_n$, $\text{O}_2(\text{H}_2\text{O})_n$, and $(\text{O}_2)_2(\text{H}_2\text{O})_n$ clusters ($10 \leq n \leq 50$) were calculated by the method of molecular dynamics using a flexible model of molecules. The frequency distribution of the power scattered by the cluster systems was obtained in the range $0 \leq \omega \leq 3000 \text{ cm}^{-1}$. The capture of one oxygen molecule by the clusters is accompanied by a decrease in the absorption of the low-frequency IR radiation and by a peak of the absorption intensity in the vicinity of $\omega 2704 \text{ cm}^{-1}$. This is also accompanied by a decrease in the reflection coefficient throughout the frequency range and a decrease in the emission power at $\omega < 1030$ and $\omega > 1700 \text{ cm}^{-1}$. Addition of two oxygen molecules to the clusters decreases the capability of the dispersions for the absorption, reflection, and scattering of IR radiation.

DOI: 10.1134/S1070363206110035

The electronic spectrum of the O_2 molecule is very important for understanding processes that occur in the upper layers of the atmosphere. Molecular oxygen strongly absorbs the solar radiation in the frequency range $(52\text{--}57) \times 10^3 \text{ cm}^{-1}$. Specifically this absorption determines the edge of absorption of UV radiation by air. In contrast to the majority of other stable diatomic molecules with the even electron number, the ground state of the O_2 molecule is not singlet but triplet [1]. Therefore, gaseous oxygen is paramagnetic. For the water molecule, owing to the presence of light hydrogen atoms, the moments of inertia are relatively low but the rotation inertia, on the contrary, is large. As a result, the frequencies of transitions between the energy levels and hence the absorption spectra are observed in the IR range. The bending frequency ν_{def} of the water molecule is 1600 cm^{-1} , and the mean stretching frequency ν_{val} , 3700 cm^{-1} .

The properties of natural water strongly depend on its oxygen content. The presence of calcium, magnesium, and other dissolved substances results in binding of a part of oxygen. The concentrations of these substances can be quite different; therefore, the properties of oxygen-saturated water can also be very diverse. Dissolved O_2 gas and calcite allow magnetization of water [2]. Molecular oxygen exhibits orientation Langevin paramagnetism which is preserved on dissolution of oxygen in water. In the presence of an external magnetic field gradient, the O_2 molecules

with the noncompensated magnetic moments tend to orient parallel to the field and to be drawn into the area with a higher magnetic field intensity. Water in the dispersed state preserves many properties of bulk water. The possibility of uptake of HCl , N_2 , Cl_2 , CO , CO_2 , N_2O , CH_4 , and CH_3OH molecules by water clusters was demonstrated by the method of molecular dynamics [3–8]. The uptake of oxygen molecules by water clusters was studied in the approximation of the rigid TIP4P water model [9]. Addition of O_2 molecules decreases the absorption coefficient of water clusters and the power of the radiation scattered by them. The effect of oxygen uptake on the spectral characteristics of water clusters should be reproduced more adequately by using the flexible model of molecules.

The goal of this work was to study, using the flexible model of molecules, the capture of molecular oxygen by water clusters and to determine how the uptake of O_2 molecules by the aqueous dispersion medium affects the IR absorption and reflection spectra and the power of the radiation emitted by the cluster systems.

Molecular-dynamic model. In this study we used the improved TIP4P model of water. The geometry of the monomer in this model is based on data for water vapor: The O–H bond length is taken as 0.09572 nm , and the H–O–H angle, as 104.5° . Fixed charges are ascribed to hydrogen atoms and to point M lying on

the bisector of the H–O–H angle at a distance of 0.0215 nm from the oxygen atom. The charge values (q_H 0.519e, q_M -1.038e) and position of point M are chosen so as to reproduce both the experimental dipole and quadrupole moments [11], on the one hand, and the energy and characteristic distances of the dimer given by ab initio calculations [12], on the other hand. The model involves calculation of the induced dipole moments of molecules, which allows the effect of their polarization to be included in the consideration. The dynamics of the molecular system is realized with the potential of water–water intermolecular interaction [13] and with the description of the oxygen–oxygen and oxygen–water interactions in the form of the sum of the repulsive and dispersion contributions [14]:

$$\Phi(r_{ij}) = b_i b_j \exp[-(c_i + c_j)r_{ij}] - a_i a_j r_{ij}^{-6},$$

where the parameters a_i , b_i , and c_i of the potential describing these interactions are taken from [15]. The interatomic distance in the O₂ molecule, r_{OO} , is taken as 0.12074 nm [16].

It is believed [17] that polarizable flexible models allow considerably better reproduction of the properties of a liquid phase. Rigorous flexible models of water cannot be particularly classical but should include in consideration the quantum degrees of freedom. However, consideration of quantum effects increases the computation volume by at least an order of magnitude and makes the simulation inefficient.

Lemberg et al. [18, 19] developed flexible models of molecules within the framework of the Hamilton dynamics. Let us consider a diatomic molecule. Let atoms A and B in the molecule be separated by a distance q :

$$q = \|\mathbf{r}_A - \mathbf{r}_B\|,$$

where r_A and r_B are vectors defining the atomic positions. Let us denote the respective atomic velocities as v_A and v_B and define the reduced weight as

$$\mu = \frac{m_A m_B}{m_A + m_B}.$$

The size of a molecule consisting of atoms A and B is determined by equilibration of the total potential force $f(q) = -\partial r / \partial q \nabla \Phi(r)$ by the centrifugal force $-\mu q \omega^2$:

$$-\mu q \omega^2 - \mathbf{f}(\mathbf{r})(\partial \mathbf{r} / \partial \mathbf{q}) = 0,$$

where $\omega = \|v_A - v_B\|/q$ is the angular velocity. By minimizing the contribution to the potential energy U from each generalized coordinate, we obtain

$$\frac{\partial}{\partial q_i} H(\mathbf{r}, \mathbf{v}) = \frac{\partial}{\partial q_i} \left(\frac{1}{2} \mu_i q_i^2 \omega_i^2 + U(\mathbf{r}) \right) = 0.$$

This method can be generalized to molecules of any composition [17].

The study of oxygen uptake by water clusters was started with the construction of a configuration of an equilibrium water cluster and oxygen molecules surrounding it. The initial equilibrium configurations of water clusters were obtained in separate molecular-dynamics calculations. In so doing, the kinetic energy of molecules constituting the clusters corresponded to a temperature of 233 K. Initially the center of gravity of the free oxygen molecules (one or two) was placed at a distance of 0.6 to 0.7 nm from the nearest atom of the water cluster, so that each atom of the oxygen molecule was in the field of molecular interaction. The cutting radius for all the interactions in the model was 0.9 nm. The linear O₂ molecule was oriented along the ray connecting its center with the center of gravity of the cluster. If there were two molecules added to the cluster, they were arranged along the same ray but on different sides of the cluster. Such a symmetrical arrangement of the molecules created conditions for the uniform effect of the admixture on the cluster and minimized the interaction between the free O₂ molecules. Equilibration of the newly formed system was performed in the time interval $0.6 \times 10^6 \Delta t$, where the time step Δt was taken as 10^{-17} s, and then the required physicochemical properties were calculated in the time interval $2 \times 10^6 \Delta t$. The equations of motion of the centers of gravity of the molecules were integrated by the fourth-order Gear method [20]. Analytical solution of the motion equations for the molecular rotation was made using the Rodrig–Hamilton parameters, and the scheme of integration of the equations of motion involving rotations corresponded to the approach suggested by Sonnenschein [22]. The computations were performed with a Pentium IV computer with a CPU speed of 3.8 GHz.

Dielectric properties. Let us consider the case of scattering of nonpolarized light when the molecular path length l is much shorter than the light wavelength λ . The extinction coefficient h of the incident beam, on the one hand, is determined by the Rayleigh formula [23] and, on the other hand, through the scattering coefficient ρ [$h = (16\pi/3)\rho$] [24] in the approximation of scattering at an angle of 90°. Taking into account that $h = \alpha + \rho$, where α is the absorption coefficient, we obtain

$$N = \frac{2\omega^4 (\sqrt{\epsilon} - 1)^2}{3\pi c^4 \alpha} \left(1 - \frac{3}{16\pi} \right),$$

where N is the number of scattering centers in 1 cm^3 ; c , light velocity; ε , dielectric permittivity of the medium; and ω , frequency of the incident wave.

Let us define the following types of ultradisperse systems:

(1) system filled by clusters of water molecules of size from 10 to 50 molecules (system I);

(2) medium consisting of $(\text{H}_2\text{O})_n$ clusters that took up one O_2 molecule each (system II);

(3) system consisting of $(\text{O}_2)_2(\text{H}_2\text{O})_n$ aggregates (system III).

Let us form system II and III in such a manner that a cluster consisting of i molecules of the admixture and n water molecules has the following statistical weight:

$$W_{in} = \frac{N_{in}}{N_{\Sigma}}, \quad i = 1, 2, n = 10, 15, \dots, 50,$$

where N_{in} is the number of clusters consisting of i molecules of admixture and n molecules of water in 1 cm^3 ; $N_{\Sigma} = \sum_{k=1}^9 N_k$; k characterizes the set of indices i, n .

For example, at $k = 1$ n is always equal to 10 and i can be 1 or 2. Similar weights were used for $(\text{H}_2\text{O})_n$ clusters forming system I. In what follows, all the spectral characteristics were calculated taking into account the assumed statistical weights W_{in} . The procedure for construction of cluster systems implies uniform distribution of these formations and is valid at low concentration of clusters when they do not interact with each other. The mean concentration of each type of clusters in the systems under consideration is lower than the Loschmidt number by 12–13 orders of magnitude.

The static dielectric permittivity ε_0 was calculated through fluctuations of the total dipole moment \mathbf{M} [25]:

$$\varepsilon_0 = 1 + \frac{4\pi}{3VkT}.$$

The dielectric permittivity $\varepsilon(\omega)$ was represented as a complex quantity $\varepsilon(\omega) = \varepsilon'(\omega) + i\varepsilon''(\omega)$, which was determined from the following equation [25, 26]:

$$\frac{\varepsilon(\omega) - 1}{\varepsilon_0 - 1} = -\int_0^{\infty} \exp(-i\omega t) \frac{dF}{dt} dt = 1 - i\omega \int_0^{\infty} \exp(-i\omega t) F(t) dt.$$

Here the function $F(t)$ is the normalized autocorrelation function of the total dipole moment of the cluster:

$$F(t) = \frac{\langle \mathbf{M}(t) \cdot \mathbf{M}(0) \rangle}{\langle \mathbf{M}^2 \rangle}.$$

The IR absorption cross section was set as follows [27]:

$$\sigma(\omega) = \left(\frac{2}{\varepsilon_v c \hbar n} \right) \omega \tan h \left(\frac{\hbar \omega}{2kT} \right) \text{Re} \int_0^{\infty} dt e^{i\omega t} \langle \mathbf{M}(t) \mathbf{M}(0) \rangle,$$

where ε_v is the dielectric permittivity of vacuum; $\hbar = h/2\pi$, where h is the Planck constant; and n is the refractive index independent on the frequency ω .

The reflection coefficient R is defined as the ratio of the mean energy flux reflected from the surface to the incident flux. At the normal incidence of a plane wave, the reflection coefficient is given by the following formula [23]:

$$R = \frac{|\sqrt{\varepsilon_1} - \sqrt{\varepsilon_2}|^2}{|\sqrt{\varepsilon_1} + \sqrt{\varepsilon_2}|^2}. \quad (1)$$

Here it is assumed that the wave incidence occurs from a transparent medium (medium 1) into a medium that can be both transparent and nontransparent, i.e., absorbing or scattering (medium 2). The indices at the dielectric permittivity in expression (1) refer to the medium.

The frequency dispersion of the dielectric permittivity determines the frequency dependence of the dielectric loss $P(\omega)$ in accordance with the following expression [24]:

$$P = \frac{\varepsilon'' \langle E^2 \rangle \omega}{4\pi},$$

where E^2 is the mean squared electric field intensity and ω is the frequency of the emitted electromagnetic wave.

Calculation results. Molecular-dynamics [28] and ab initio [29] calculations were performed to determine the structure of water clusters characterized by the minimal energy. With an increase in the cluster size, the results obtained using different models become appreciably different. For example, for the $(\text{H}_2\text{O})_{20}$ cluster, the difference between the energies of the most favorable structures according to POL1 [30] and SPC/E [31] models is 13.4%. In our model, the energy of the $(\text{H}_2\text{O})_{20}$ cluster at $T = 233 \text{ K}$, 8.66 eV, is intermediate between the values given by the POL1 and SPC/E models. The structures of the clusters also differ significantly. Whereas the POL1 model gave for the cluster the shape of a cell consisting of four-, five-, and six-unit rings, in the SPC/E model the

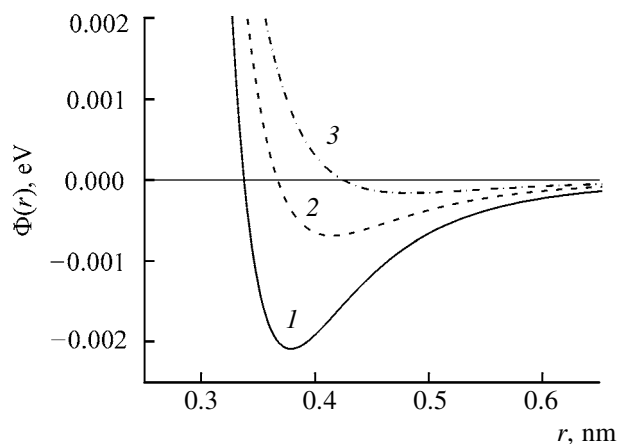


Fig. 1. Interaction potentials of atomic pairs: (1) O–O, (2) O–H, and (3) H–H.

structure with the minimal energy is a pentagonal prism. In our model, the minimum-energy structure of the $(\text{H}_2\text{O})_{20}$ cluster is a strongly distorted pentagonal dodecahedron. Introduction of the polarizability and of flexible bonds leads to a decrease in the energy of the system of strained hydrogen bonds.

The potentials used for the pairs (O–O, O–H, H–H) of interacting atoms are shown in Fig. 1. Each of these potentials has the ranges of attraction and repulsion. The transition from repulsion to attraction is observed at 0.34, 0.37, and 0.42 nm for the atomic pairs O–O, O–H, and H–H, respectively. The steepest repulsion branch is observed for the O–O pair, and the least steep branch, for the H–H pair. The initial distance between the O_2 molecules from the $(\text{H}_2\text{O})_n$ clusters was so that the r_{OO} and r_{OH} distances between different molecules were no less than 0.6 nm. Hence, under the action of attraction forces the O_2 molecule moved from its initial position toward the water cluster and either stopped and was subsequently retained at a certain distance from the cluster, or directly adhered to its surface. The configurations of the $(\text{H}_2\text{O})_{50}$ cluster that took up one and two O_2 molecules are shown in Fig. 2. In both cases, the O_2 molecules in the course of the calculation are oriented tangentially to the cluster surface. The single O_2 molecule is attracted more strongly and fits in the cluster surface, whereas with a pair of O_2 molecules only one of them virtually adheres to the surface and the other molecule is arranged at a certain distance from it. The oxygen molecules are retained at a water cluster owing to attraction by the hydrogen atoms that are oriented toward the oxygen molecule and belong to one or several water molecules on the cluster surface. The limited solubility of molecular oxygen in an aqueous dispersion medium is thus manifested.

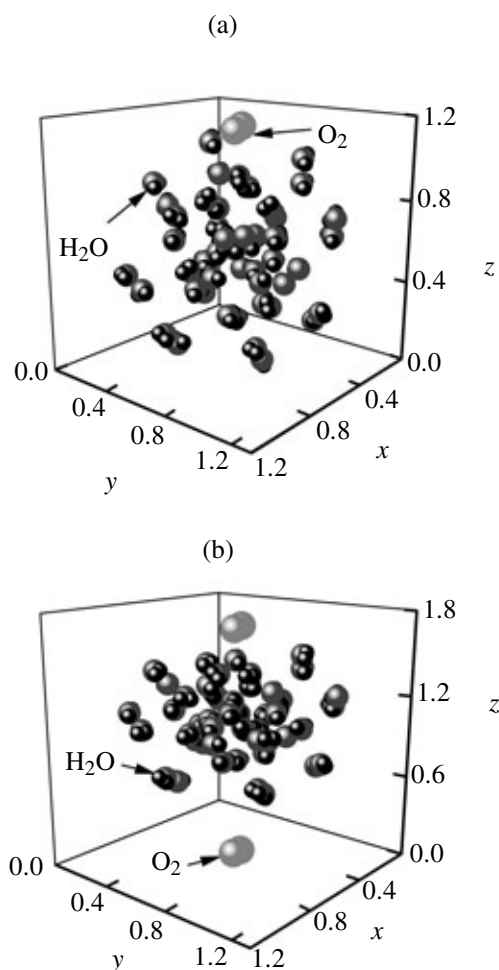


Fig. 2. Configurations of the clusters (a) $\text{O}_2(\text{H}_2\text{O})_{50}$ and (b) $(\text{O}_2)_2(\text{H}_2\text{O})_{50}$ corresponding to a time moment of 20 ps. The molecular coordinates are given in nm.

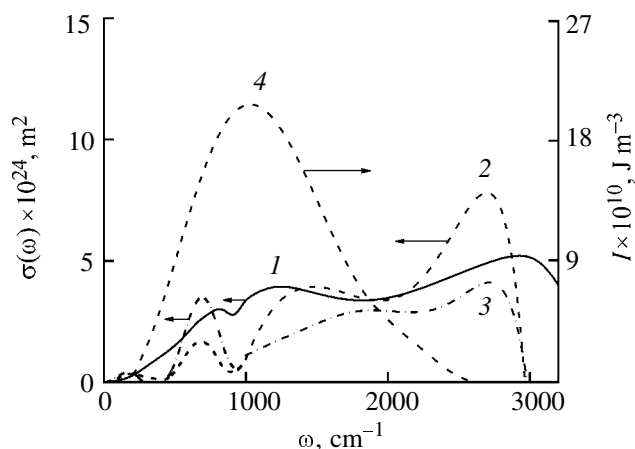


Fig. 3. IR absorption spectra of systems (1) I, (2) II, and (3) III (left ordinate); (4) spectrum of the thermal radiation of the Earth at $T = 280$ K (right ordinate).

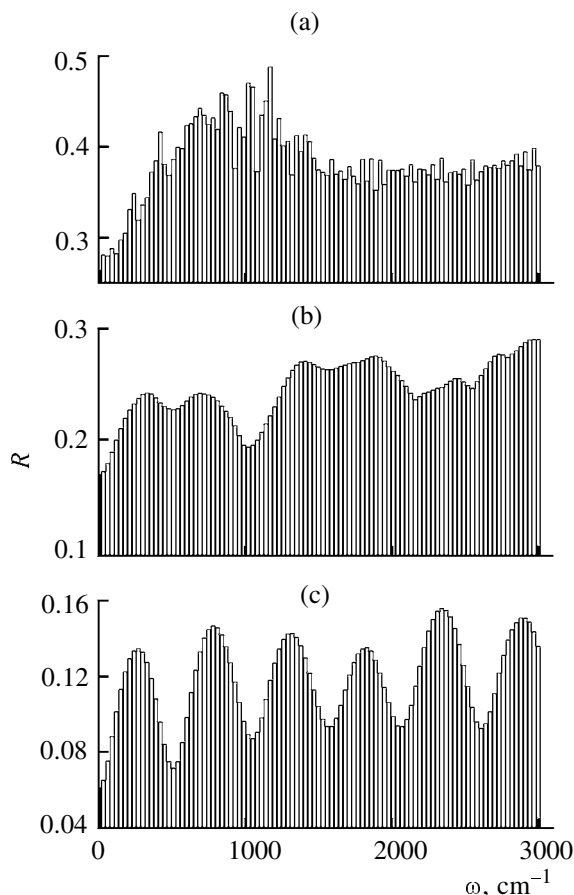


Fig. 4. Coefficient of reflection of a monochromatic plane electromagnetic wave by cluster systems (a) I, (b) II, and (c) III.

When O_2 molecules are arranged on different sides of the $(\text{H}_2\text{O})_{50}$ cluster, the cluster becomes ellipsoidal, with the minor axis parallel to the line connecting the O_2 molecules taken up.

The IR absorption by aqueous dispersions was considered in the frequency range $0 \leq \omega \leq 3000 \text{ cm}^{-1}$ covering the spectrum of the thermal radiation of the Earth (Fig. 3). Note that this range involves both the absorption range associated with the molecular vibrations ($\omega > 1000 \text{ cm}^{-1}$) and the range of absorption originating from intramolecular bending vibrations and librations [32]. The maximum of the IR radiation of the Earth (ω_g 1060 cm^{-1} , T 280 K) is close to the second maximum (ω_2 1150 cm^{-1}) of system I for straight water. The cross section of the IR absorption by system I has a weakly pronounced peak in the vicinity of ω_1 786 cm^{-1} . As a result of absorption of thermal radiation, this peak becomes well-resolved and shifts toward far-IR range for systems II and III (ω_1 680 and 690 cm^{-1} , respectively). The uptake of one oxygen molecule per water cluster (system II) results in a decrease in the absorption of the IR radia-

tion of the Earth, especially at lower frequencies ($\omega < 1600 \text{ cm}^{-1}$). The absorption of the Earth's radiation becomes still weaker upon uptake of two oxygen molecules per water cluster (system III). In this case, too, the low-frequency radiation ($\omega \leq 1000 \text{ cm}^{-1}$) is absorbed more weakly. At higher frequencies, on the contrary, moderate oxygen uptake (one O_2 molecule per water cluster) strongly enhances the IR absorption at ω_3 2704 cm^{-1} . The intensity of the third peak of the absorption cross section for system II even exceeds that of the corresponding peak for system I, i.e., for the dispersion medium consisting of straight water. However, the intensity of the Earth's radiation at frequencies corresponding to this absorption peak is extremely low. The IR absorption at ω_3 2704 cm^{-1} is also enhanced in system III, but the intensity of the second peak in this system is weaker compared to the absorption by system I.

The reflection spectrum of a plane monochromatic electromagnetic wave undergoes strong changes upon uptake of oxygen molecules by the aqueous dispersion medium (Fig. 4). For system I (straight dispersed water), the strongest reflection is observed in the frequency range $400 \leq \omega \leq 1400 \text{ cm}^{-1}$. The reflection coefficient R in this case reaches 0.48 at ω 1170 cm^{-1} . The pattern changes essentially upon uptake of one O_2 molecule per water cluster. Certain peaks appeared in the continuous spectrum $R(\omega)$ of system II; the mean value \bar{R} decreased from 0.38 (system I) to 0.24 (II). Uptake of one more O_2 molecule per water cluster further decreased \bar{R} to 0.12, and six well-resolved peaks appeared in the $R(\omega)$ spectrum. The strongest peak is observed at 2340 cm^{-1} .

The power of the emission of the energy accumulated by dispersions also strongly depends on the presence of oxygen (Fig. 5a). In the case of the dispersion of straight water, the first scattered power peak is observed at ω 685 cm^{-1} , and in the case of systems II and III, at ω 780 and 840 cm^{-1} , respectively. The intensities of this peak of the functions $P_{\text{II}}(\omega)$ and $P_{\text{III}}(\omega)$ for systems II and III containing oxygen are considerably weaker than for system I. In the region of high frequencies, there is one more maximum of the $P(\omega)$ spectrum for systems I and III and two more maxima for system II. The second maxima for systems I and III correspond to the frequencies of 2920 and 2540 cm^{-1} , and the high-frequency maxima of this spectrum for system II are localized at 1970 and 2920 cm^{-1} . On the whole, oxygen uptake by aqueous dispersion results in a considerable decrease in the emission power. The rate of the energy dissipation continues to decrease with an increase in the O_2 concentration in the dispersion. The integral intensities of the emission power for systems I, II, and III are in a ratio of $1 : 0.5 : 0.3$. However, there is a frequency

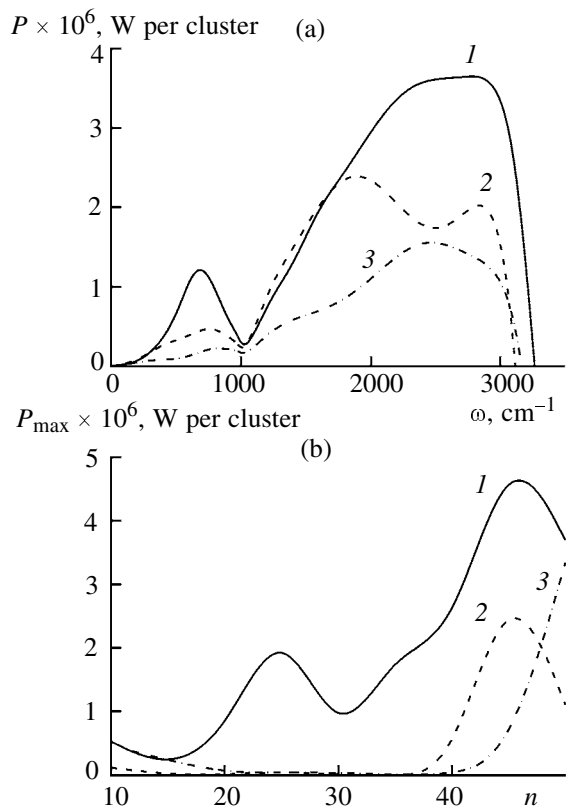


Fig. 5. (a) Frequency dependence $P(\omega)$ of the IR emission power for systems (1) I, (2) II, and (3) III, and (b) dependence of the maximal value of P on the number of water molecules n in clusters (1) $(\text{H}_2\text{O})_n$, (2) $\text{O}_2(\text{H}_2\text{O})_n$, and (3) $(\text{O}_2)_2(\text{H}_2\text{O})_n$.

range $1030 \leq \omega \leq 1700 \text{ cm}^{-1}$ in which $P_{\text{II}} \geq P_{\text{I}}$. Figure 5b shows how the strongest emission power is distributed within each dispersion. For systems I and II, the maximal emission power is exhibited by clusters consisting of 45 water molecules, and for system III, by the aggregate $(\text{O}_2)_2(\text{H}_2\text{O})_{50}$. The straight water cluster consisting of 25 molecules also exhibits relatively high rate of energy dissipation.

Thus, enrichment of aqueous dispersions in oxygen significantly affects the absorption, reflection, and scattering of the IR energy by these systems. On the whole, absorption of the Earth's thermal radiation by aqueous dispersions is weakened owing to capture of molecular oxygen. This is due to the fact that, in the frequency range of the active Earth's radiation, the integral IR absorption decreases upon oxygen uptake. On the contrary, at high frequencies, water clusters with one oxygen molecule show a stronger capability for IR absorption, but the intensity of the Earth's radiation in this range is extremely low. The presence of molecular oxygen in aqueous dispersions significantly

alters the IR reflection spectra of these systems. Firstly, the effective reflection coefficient decreases with increasing oxygen concentration in the dispersion. Secondly, as the O_2 concentration increases, the continuous spectrum gradually transforms into a band spectrum. The scattering of the accumulated thermal energy by an aqueous dispersion weakens with increasing oxygen content of the dispersion. The thermal emission power is largely determined by the cluster structure and is not a monotonic function of its size.

ACKNOWLEDGMENTS

The study was financially supported by the Russian Foundation for Basic Research (project no. 04-02-17322).

REFERENCES

1. El'yashevich, M.A., *Atomnaya i molekulyarnaya spektroskopiya (Atomic and Molecular Spectroscopy)*, Moscow: Gos. Izd. Fiziko-Matematicheskoi Literatury, 1962.
2. Chibowski, E., Holysz, L., Szczes, A., and Chibowski, M., *Water Sci. Technol.*, 2004, vol. 49, no. 2, p. 169.
3. Galashev, A.E., Pozharskaya, G.I., and Chukanov, V.N., *Kolloidn. Zh.*, 2002, vol. 64, no. 6, p. 762.
4. Galashev, A.E., Pozharskaya, G.I., and Chukanov, V.N., *Zh. Obshch. Khim.*, 2003, vol. 73, no. 6, p. 881.
5. Galashev, A.E., Chukanov, V.N., and Pozharskaya, G.I., *Khim. Fiz.*, 2001, vol. 20, no. 9, p. 8.
6. Galashev, A.E. and Chukanov, V.N., *Kolloidn. Zh.*, 2004, vol. 66, no. 5, p. 588.
7. Galashev, A.E., Rakhmanova, O.R., and Chukanov, V.N., *Kolloidn. Zh.*, 2005, vol. 67, no. 3, p. 308.
8. Brodskaya, E.N., *Kolloidn. Zh.*, 2001, vol. 63, no. 1, p. 10.
9. Galashev, A.E., Chukanov, V.N., and Galasheva, O.A., *Kolloidn. Zh.*, 2006, vol. 68, no. 2, p. 155.
10. Dang, L.X. and Chang, T.-M., *J. Chem. Phys.*, 1997, vol. 106, no. 19, p. 8149.
11. Xantheas, S., *J. Chem. Phys.*, 1996, vol. 104, no. 21, p. 8821.
12. Smith, D.E. and Dang, L.X., *J. Chem. Phys.*, 1994, vol. 100, no. 5, p. 3757.
13. Galashev, A.E., Rakhmanova, O.R., and Chukanov, V.N., *Khim. Fiz.*, 2005, vol. 24, no. 3, p. 90.
14. Spackman, M.A., *J. Chem. Phys.*, 1986, vol. 85, no. 11, p. 6579.
15. Spackman, M.A., *J. Chem. Phys.*, 1986, vol. 85, no. 11, p. 6587.

16. *Spravochnik khimika* (Chemist's Handbook), Nikol'skii, B.P., Ed., Leningrad: Khimiya, 1971, vol. 1.
17. Saint-Martin, H., Hess, B., and Berendsen, H.J.C., *J. Chem. Phys.*, 2004, vol. 120, no. 23, p. 11 133.
18. Lemberg, H.L. and Stillinger, F.H., *J. Chem. Phys.*, 1975, vol. 62, no. 5, p. 1677.
19. Rahman, A., Stillinger, F.H., and Lemberg, H.L., *J. Chem. Phys.*, 1975, vol. 63, no. 12, p. 5223.
20. Haile, J.M., *Molecular Dynamics Simulation. Elementary Methods*, New York: Wiley, 1992.
21. Koshlyakov, V.N., *Zadachi dinamiki tverdogo tela i prikladnoi teorii giroskopov* (Problems of Solid State Dynamics and Applied Gyroscope Theory), Moscow: Nauka, 1985.
22. Sonnenschein, R., *J. Comput. Phys.*, 1985, vol. 59, no. 3, p. 347.
23. Landau, L.D. and Lifshits, E.M., *Elektrodinamika sploshnykh sred* (Electrodynamics of Continuous Media), Moscow: Nauka, 1982, vol. 8.
24. *Fizicheskaya entsiklopediya* (Physical Encyclopedia), Prokhorov, A.M., Ed., Moscow: Sov. Entsiklopediya, 1988, vol. 1.
25. Bresme, F., *J. Chem. Phys.*, 2001, vol. 115, no. 16, p. 7564.
26. Neumann, M., *J. Chem. Phys.*, 1985, vol. 82, no. 12, p. 5663.
27. Bosma, W.B., Fried, L.E., and Mukamel, S., *J. Chem. Phys.*, 1993, vol. 98, no. 6, p. 4413.
28. Sremaniak, L.S., Perera, L., and Berkowitz, M.L., *J. Chem. Phys.*, 1996, vol. 105, no. 9, p. 3715.
29. Tsai, C.J. and Jordan, K.D., *J. Phys. Chem.*, 1993, vol. 97, no. 20, p. 5207.
30. Dang, L.X. and Garrett, B.C., *J. Chem. Phys.*, 1993, vol. 99, no. 4, p. 2972.
31. Berendsen, H.J.C., Grigera, J.R., and Straatsman, T.P., *J. Phys. Chem.*, 1987, vol. 91, no. 24, p. 6269.
32. <http://pigseye.kennesaw.edu/~jdumas/IR2-3.html>.